Test Bench - Amplified Piezoelectric Actuator

Dehaeze Thomas

March 22, 2024

Contents

Figure 1: Picture of 5 out of the 7 received APA300ML

The first goal is to characterize the APA300ML in terms of:

- The, geometric features, electrical capacitance, stroke, hysteresis, spurious resonances. This is performed in Section 1.

- The dynamics from the generated DAC voltage (going to the voltage amplifiers and then applied on the actuator stacks) to the induced displacement, and to the measured voltage by the force sensor stack. Also the "actuator constant" and "sensor constant" are identified. This is done in Section 2.

- Compare the measurements with the Simscape models (2DoF, Super-Element) in order to tuned/-validate the models. This is explained in Section **??**.

Table 1: Report sections and corresponding Matlab files

Sections	Matlab File
Section 1	`test_apa_1_basic_meas.m`
Section 2	`test_apa_2_dynamics.m`
Section 3	`test_apa_3_model_2dof.m`
Section 4	`test_apa_4_model_flexible.m`

1 First Basic Measurements

Before using the measurement bench to characterize the APA300ML, first simple measurements are performed:

- Section 1.1: the geometric tolerances of the interface planes are checked

- Section 1.2: the capacitance of the piezoelectric stacks is measured

- Section 1.3: the stroke of each APA is measured

- Section 1.4: the "spurious" resonances of the APA are investigated

1.1 Geometrical Measurements

To measure the flatness of the two mechanical interfaces of the APA300ML, a small measurement bench is installed on top of a metrology granite with very good flatness.

As shown in Figure 1.1, the APA is fixed to a clamp while a measuring probe[1] is used to measure the height of 4 points on each of the APA300ML interfaces.

From the X-Y-Z coordinates of the measured 8 points, the flatness is estimated by best fitting[2] a plane through all the points.

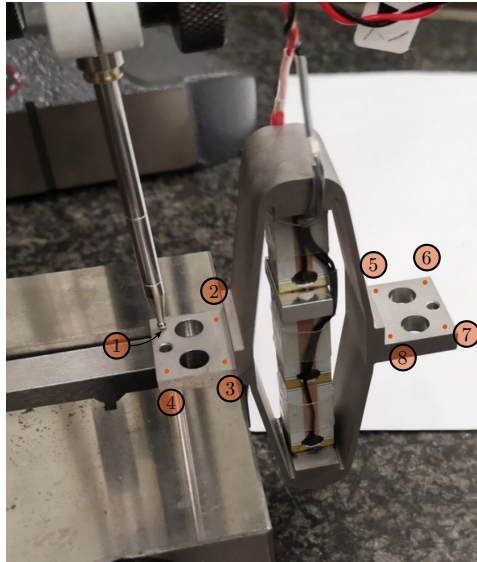The measured flatness, summarized in Table 1.1, are within the specifications.

Table 1.1: Estimated flatness of the APA300ML interfaces

	Flatness $[\mu m]$
APA 1	8.9
APA 2	3.1
APA 3	9.1
APA 4	3.0
APA 5	1.9
APA 6	7.1
APA 7	18.7

---

[1] Heidenhain MT25, specified accuracy of $0.5\,\mu m$

[2] The Matlab `fminsearch` command is used to fit the plane

Figure 1.1: Measurement setup for flatness estimation of the two mechanical interfaces

1.2 Electrical Measurements

From the documentation of the APA300ML, the total capacitance of the three stacks should be between $18\,\mu F$ and $26\,\mu F$ with a nominal capacitance of $20\,\mu F$.

The capacitance of the piezoelectric stacks found in the APA300ML have been measured with the LCR meter[3] shown in Figure 1.2. The two stacks used as an actuator and the stack used as a force sensor are measured separately.
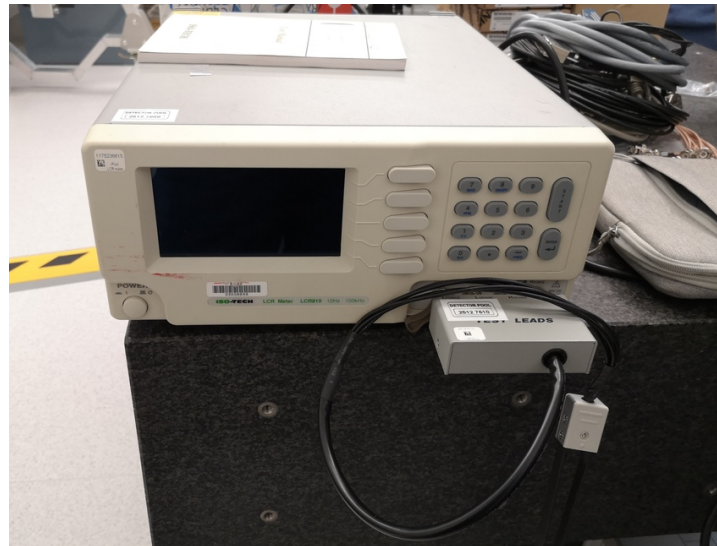
Figure 1.2: LCR Meter used for the measurements

The measured capacitance are summarized in Table 1.2 and the average capacitance of one stack is

---

[3]LCR-819 from Gwinstek, specified accuracy of 0.05%, measured frequency is set at $1\,kHz$

$\approx 5\mu F$. However, the measured capacitance of the stacks of "APA 3" is only half of the expected capacitance. This may indicate a manufacturing defect.

The measured capacitance is found to be lower than the specified one. This may be due to the fact that the manufacturer measures the capacitance with large signals ($-20\,V$ to $150\,V$) while it was here measured with small signals.

Table 1.2: Capacitance measured with the LCR meter. The excitation signal is a sinus at 1kHz

	Sensor Stack	Actuator Stacks
APA 1	5.10	10.03
APA 2	4.99	9.85
APA 3	1.72	5.18
APA 4	4.94	9.82
APA 5	4.90	9.66
APA 6	4.99	9.91
APA 7	4.85	9.85

1.3 Stroke and Hysteresis Measurement

The goal is here to verify that the stroke of the APA300ML is as specified in the datasheet. To do so, one side of the APA is fixed to the granite, and a displacement probe[4] is located on the other side as shown in Figure 1.3.

Then, the voltage across the two actuator stacks is varied from $-20\,V$ to $150\,V$ using a DAC and a voltage amplifier. Note that the voltage is here slowly varied as the displacement probe has a very low measurement bandwidth (see Figure 1.3, left).

The measured APA displacement is shown as a function of the applied voltage in Figure 1.4, right.

Typical hysteresis curves for piezoelectric stack actuators can be observed. The measured stroke is approximately $250\,\mu m$ when using only two of the three stacks, which is enough for the current application. This is even above what is specified as the nominal stroke in the data-sheet ($304\,\mu m$, therefore $\approx 200\,\mu m$ if only two stacks are used).

It is clear from Figure 1.4 that "APA 3" has an issue compared to the other units. This confirms the abnormal electrical measurements made in Section 1.2. This unit was send sent back to Cedrat and a new one was shipped back. From now on, only the six APA that behave as expected will be used.
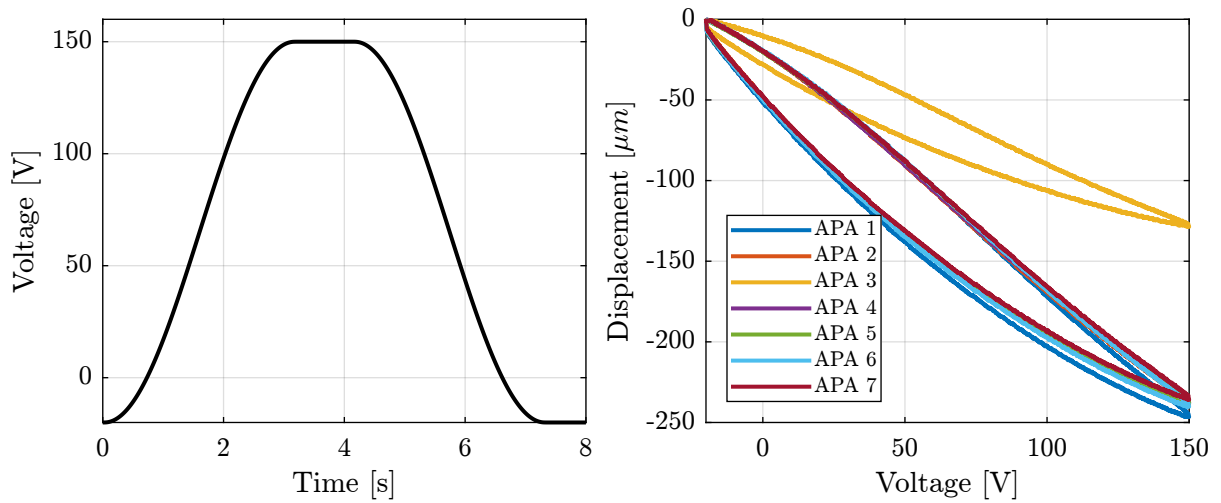
1.4 Flexible Mode Measurement

In this section, the flexible modes of the APA300ML are investigated both experimentally and using a Finite Element Model.

---

[4]Millimar 1318 probe, specified linearity better than $1\,\mu m$
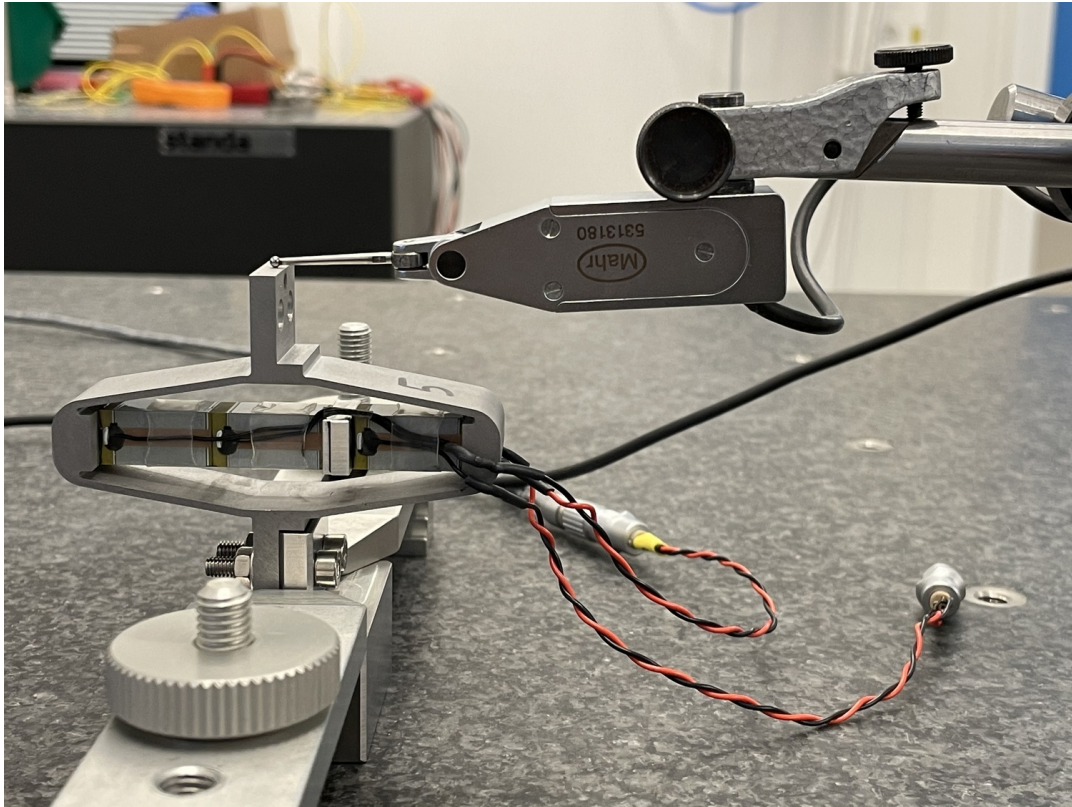
Figure 1.3: Bench to measured the APA stroke

Figure 1.4: Generated voltage across the two piezoelectric stack actuators to estimate the stroke of the APA300ML (left). Measured displacement as a function of the applied voltage (right)

To experimentally estimate these modes, the APA is fixed on one end (see Figure 1.6). A Laser Doppler Vibrometer[5] is used to measure the difference of motion between two "red" points (i.e. the torsion of the APA along the vertical direction) and an instrumented hammer[6] is used to excite the flexible modes. Using this setup, the transfer function from the injected force to the measured rotation can be computed in different conditions and the frequency and mode shapes of the flexible modes can be estimated.

The flexible modes for the same condition (i.e. one mechanical interface of the APA300ML fixed) are estimated using a finite element software and the results are shown in Figure 1.5.
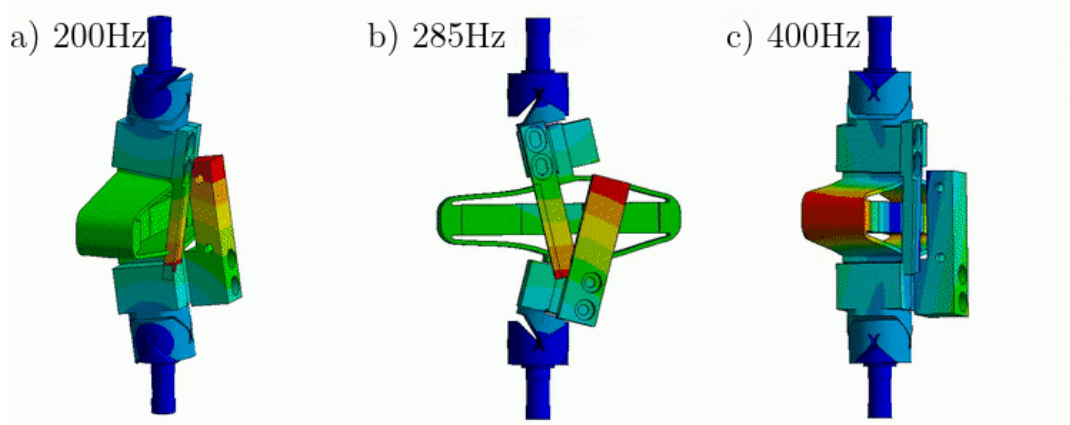
Figure 1.5: Spurious resonances - Change this with the updated FEM analysis of the APA300ML
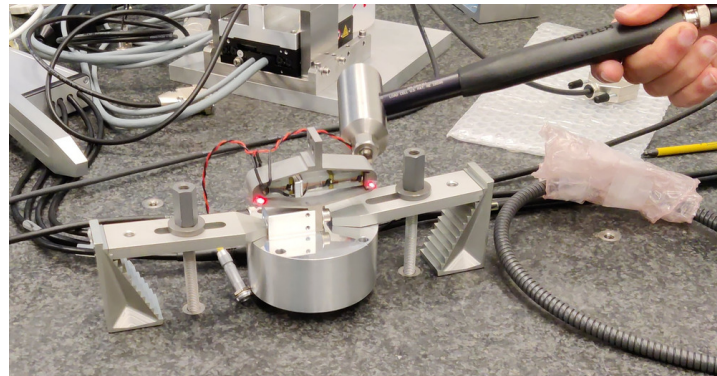
Figure 1.6: Measurement setup with a Laser Doppler Vibrometer and one instrumental hammer. Here the Z torsion is measured.

Two other similar measurements are performed to measured the bending of the APA around the X direction and around the Y direction (see Figure 1.7).
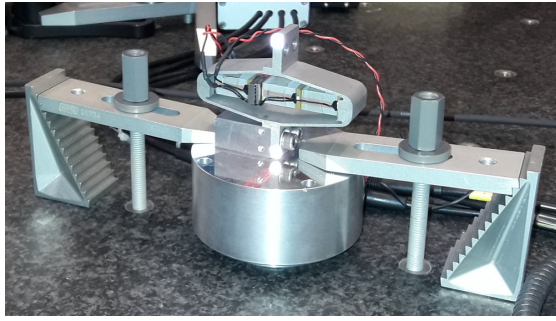
The three measured frequency response functions are shown in Figure 1.8.

- a clear x bending mode at $280\,\text{Hz}$

- a clear y bending mode at $412\,\text{Hz}$

---

[5]Polytec controller 3001 with sensor heads OFV512
[6]Kistler 9722A

(a) X bending
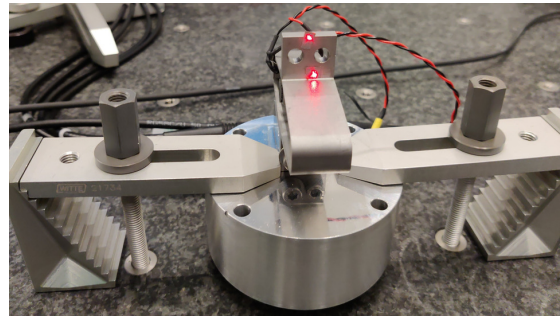
(b) Y Bending

Figure 1.7: Experimental setup to measured flexible modes of the APA300ML. For the bending in the X direction, the impact point is located at the back of the top measurement point. For the bending in the Y direction, the impact point is located on the back surface of the top interface (on the back of the 2 measurements points).

- for the z torsion test, the y bending mode is also excited and observed, and we may see a mode at $800\,\mathrm{Hz}$
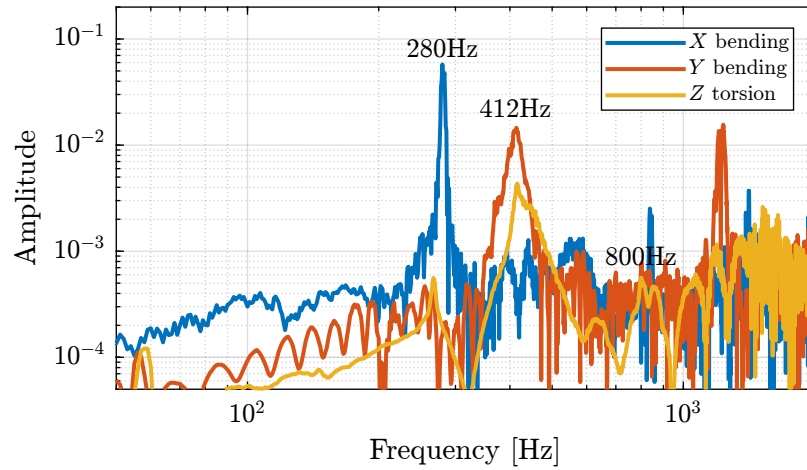
Figure 1.8: Obtained frequency response functions for the 3 tests with the instrumented hammer

Table 1.3: Measured frequency of the modes

Mode	FEM	Measured Frequency
X bending		280Hz
Y bending		410Hz
Z torsion		800Hz

2 Dynamical measurements

After the basic measurements on the APA were performed in Section 1, a new test bench is used to better characterize the APA.

This test bench is shown in Figure 2.1 and consists of the APA300ML fixed on one end to the fixed granite, and on the other end to the 5kg granite vertically guided with an air bearing. An encoder is used to measure the relative motion between the two granites (i.e. the displacement of the APA).

The bench is schematically shown in Figure 2.2 and the signal used are summarized in Table 2.1.

Table 2.1: Variables used during the measurements

Variable	Description	Unit
u	Output DAC Voltage	V
V_a	Output Amplifier Voltage	V
V_s	Measured Stack Voltage (ADC)	V
d_e	Encoder Measurement	m

This bench will be used to:

- measure the dynamics of the APA (from V_a to d_e and d_a in Section **??**, and from V_a to V_s in section **??**)

- estimate the added damping using Integral Force Feedback (Section 2.5)

These measurements will also be used to tune the model of the APA in Section **??**.

2.1 Hysteresis

As the payload is vertically guided without friction, the hysteresis of the APA can be estimated from the motion of the payload.

A quasi static sinusoidal excitation V_a with an offset of $65\,V$ (halfway between $-20\,V$ and $150\,V$), and an amplitude varying from $4\,V$ up to $80\,V$.

For each excitation amplitude, the vertical displacement d_e of the mass is measured and displayed as a function of the applied voltage..

The measured displacements as a function of the output voltages are shown in Figure 2.3. It is interesting to see that the hysteresis is increasing with the excitation amplitude.
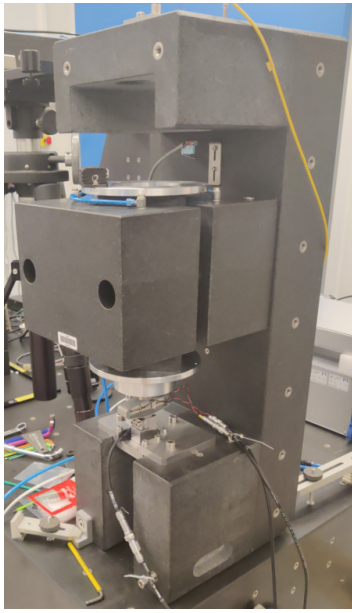
(a) Picture of the test bench
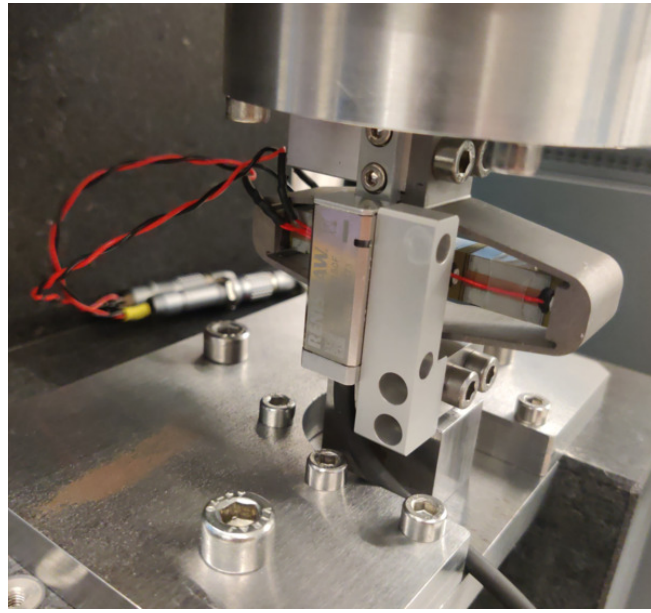
(b) Zoom on the APA with the encoder

Figure 2.1: Test bench used to characterize the APA300ML

Figure 2.2: Schematic of the Test Bench

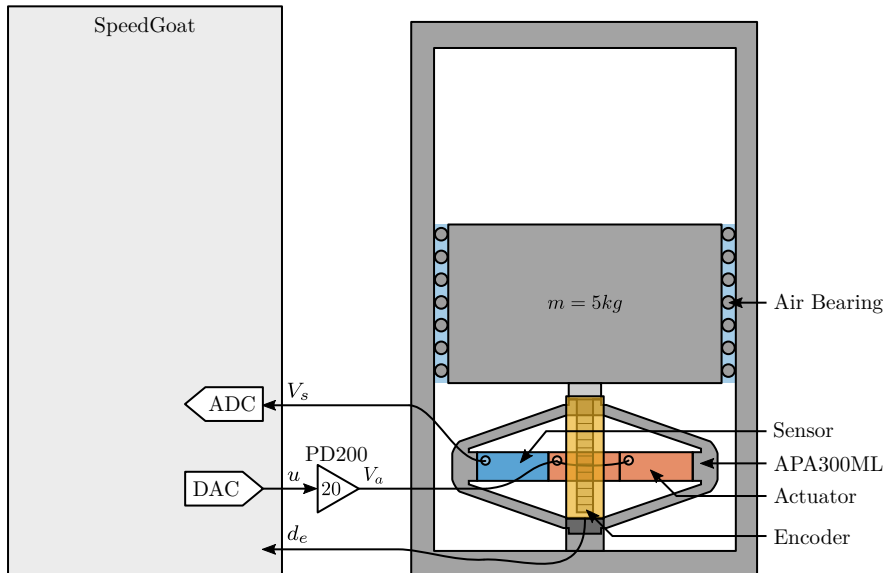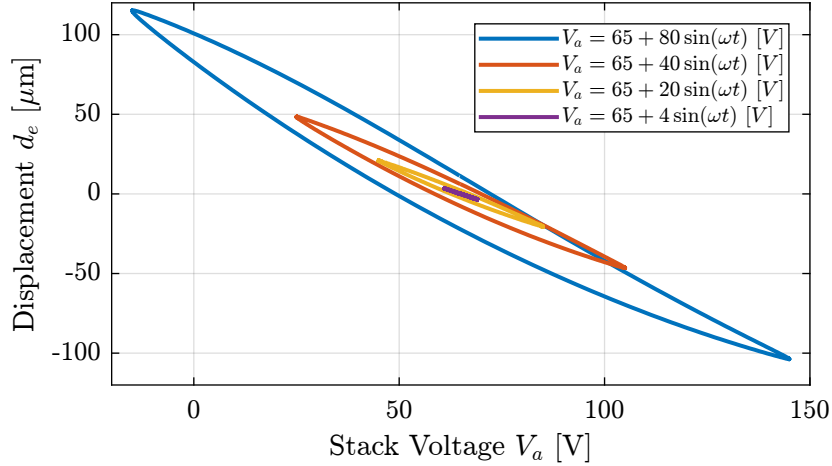**Figure 2.3:** Obtained hysteresis curves (displacement as a function of applied voltage) for multiple excitation amplitudes

2.2 Axial stiffness

In order to estimate the stiffness of the APA, a weight with known mass $m_a = 6.4\,\text{kg}$ is added on top of the suspended granite and the deflection d_e is measured using the encoder.

The APA stiffness can then be estimated from equation (2.1).

$$k_{\text{apa}} = \frac{m_a g}{\Delta d_e} \tag{2.1}$$

The measured displacement d_e as a function of time is shown in Figure 2.4. It can be seen that there are some drifts in the measured displacement (probably due to piezoelectric creep) and the that displacement does not come back to the initial position after the mass is removed (probably due to piezoelectric hysteresis). These two effects induce some uncertainties in the measured stiffness.

The stiffnesses are computed for all the APA from the two displacements d_1 and d_2 (see Figure 2.4) leading to two stiffness estimations k_1 and k_2. These estimated stiffnesses are summarized in Table 2.2 and are found to be close to the nominal stiffness $k = 1.8\,N/\mu m$ found in the APA300ML manual.

Table 2.2: Measured stiffnesses (in $N/\mu m$)

APA	k_1	k_2
1	1.68	1.9
2	1.69	1.9
4	1.7	1.91
5	1.7	1.93
6	1.7	1.92
8	1.73	1.98

The stiffness can also be computed using equation (2.2) by knowing the main vertical resonance frequency $\omega_z \approx 95\,\text{Hz}$ (estimated by the dynamical measurements shown in section 2.3) and the suspended
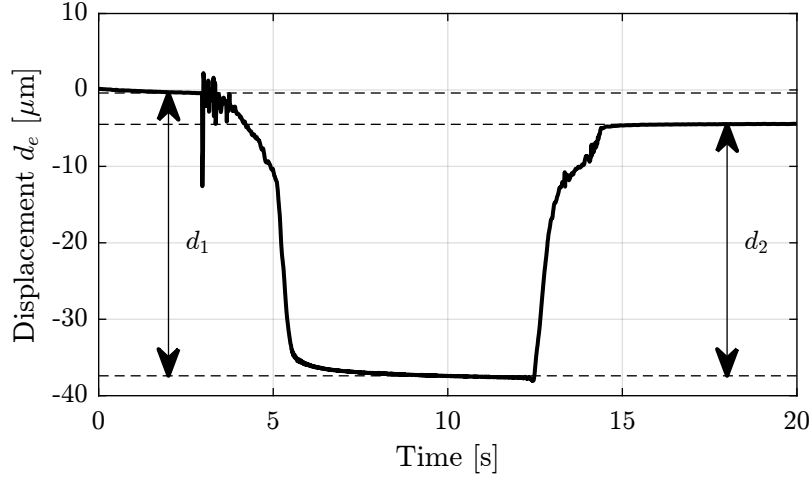
Figure 2.4: Measured displacement when adding the mass (at $t \approx 3\,s$) and removing the mass(at $t \approx 13\,s$)

mass $m_{\text{sus}} = 5.7\,\text{kg}$.

$$\omega_z = \sqrt{\frac{k}{m_{\text{sus}}}} \tag{2.2}$$

The obtain stiffness is $k \approx 2\,N/\mu m$ which is close to the values found in the documentation and by the "static deflection" method.

However, changes in the electrical impedance connected to the piezoelectric stacks impacts the mechanical compliance (or stiffness) of the piezoelectric stack [1, chap. 2].

To estimate this effect, the stiffness of the APA if measured using the "static deflection" method in two cases:

- k_{os}: piezoelectric stacks left unconnected (or connect to the high impedance ADC)

- k_{sc}: piezoelectric stacks short circuited (or connected to the voltage amplifier with small output impedance)

The open-circuit stiffness is estimated at $k_{\text{oc}} \approx 2.3\,N/\mu m$ and the closed-circuit stiffness $k_{\text{sc}} \approx 1.7\,N/\mu m$.

2.3 Dynamics

In this section, the dynamics of the system from the excitation voltage u to encoder measured displacement d_e and to the force sensor voltage V_s is identified.

The obtained transfer functions for the 6 APA between the excitation voltage u and the encoder displacement d_e are shown in Figure 2.5. The obtained transfer functions are close to a mass-spring-damper system. The following can be observed:

- A "stiffness line" indicating a static gain equal to $\approx -17\,\mu m/V$. The minus sign comes from the fact that an increase in voltage stretches the piezoelectric stack that then reduces the height of the APA

- A lightly damped resonance at $95\,\text{Hz}$

- A "mass line" up to $\approx 800\,\text{Hz}$, above which some resonances appear. These additional resonances might be coming from the limited stiffness of the encoder support or from the limited compliance of the APA support.
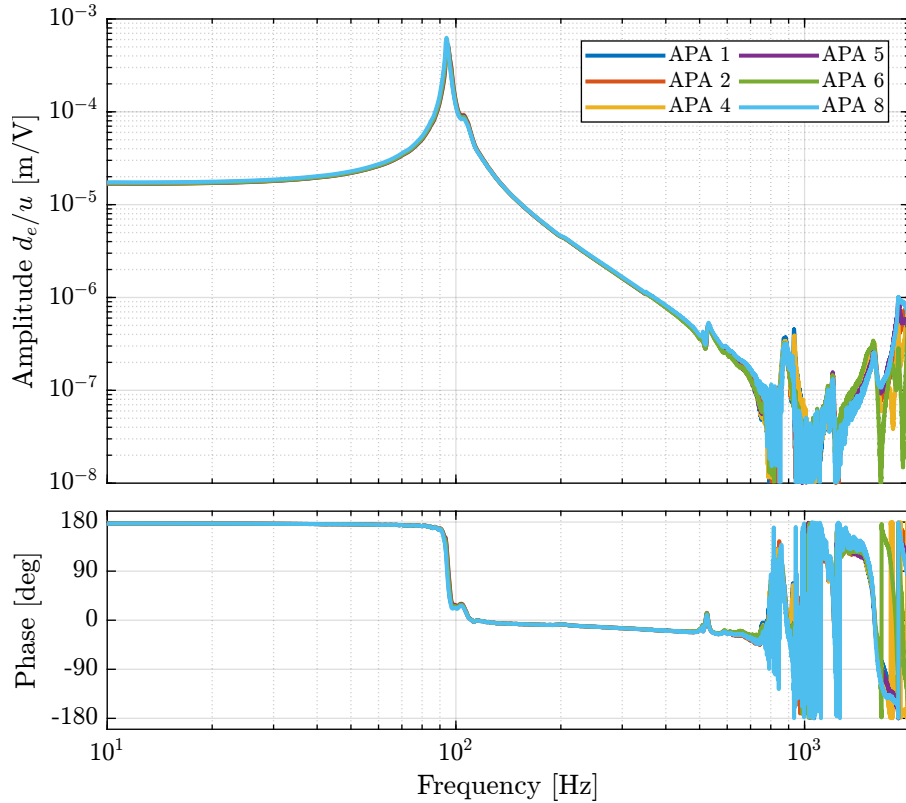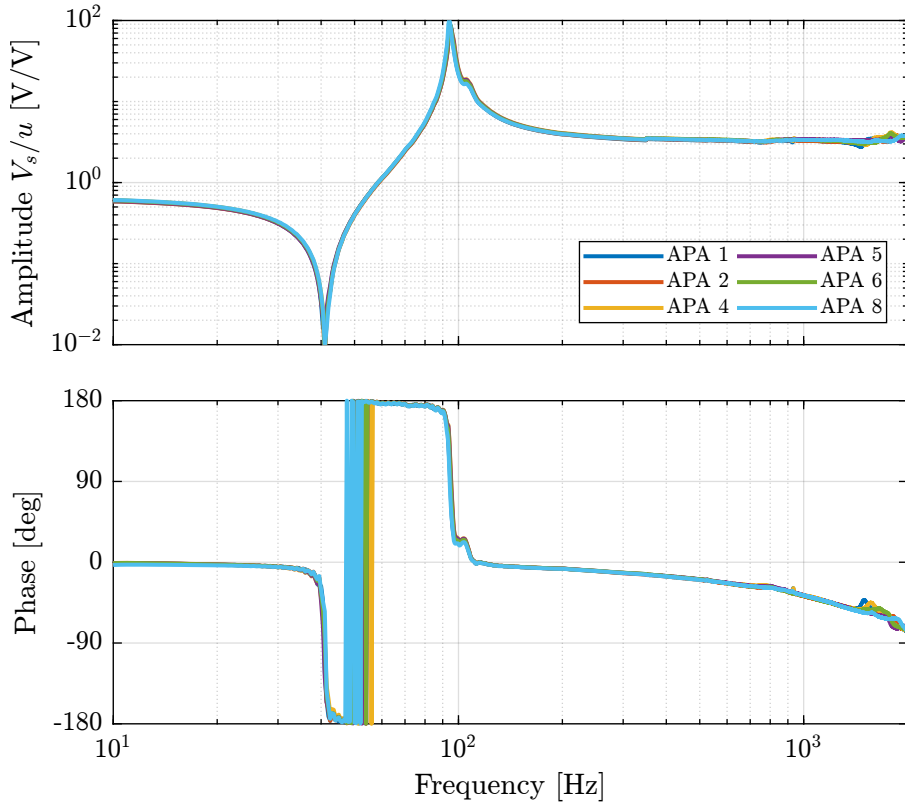

Figure 2.5: Estimated Frequency Response Function from generated voltage u to the encoder displacement d_e for the 6 APA300ML

The dynamics from u to the measured voltage across the sensor stack V_s is also identified and shown in Figure 2.6.

A lightly damped resonance is observed at $95\,\text{Hz}$ and a lightly damped anti-resonance at $41\,\text{Hz}$. No additional resonances is present up to at least $2\,\text{kHz}$ indicating at Integral Force Feedback can be applied without stability issues from high frequency flexible modes.

As illustrated by the Root Locus, the poles of the closed-loop system converges to the zeros of the open-loop plant. Suppose that a controller with a very high gain is implemented such that the voltage V_s across the sensor stack is zero. In that case, because of the very high controller gain, no stress and strain is present on the sensor stack (and on the actuator stacks are well, as they are both in series). Such closed-loop system would therefore virtually corresponds to a system for which the piezoelectric stacks have been removed and just the mechanical shell is kept. From this analysis, the axial stiffness of the shell can be estimated to be $k_{\text{shell}} = 5.7 \cdot (2\pi \cdot 41)^2 = 0.38\,N/\mu m$. Such reasoning can lead to

very interesting insight into the system just from an open-loop identification.

Figure 2.6: Estimated Frequency Response Function from generated voltage u to the sensor stack voltage V_s for the 6 APA300ML

All the identified dynamics of the six APA300ML (both when looking at the encoder in Figure 2.5 and at the force sensor in Figure 2.6) are almost identical, indicating good manufacturing repeatability for the piezoelectric stacks and the mechanical lever.

2.4 Effect of the resistor on the IFF Plant

A resistor $R \approx 80.6\,k\Omega$ is added in parallel with the sensor stack which has the effect to form a high pass filter with the capacitance of the stack.

As explain before, this is done for two reasons:

1. Limit the voltage offset due to the input bias current of the ADC

2. Limit the low frequency gain

The (low frequency) transfer function from u to V_s with and without this resistor have been measured and are compared in Figure 2.7. It is confirmed that the added resistor as the effect of adding an high pass filter with a cut-off frequency of $\approx 0.35\,Hz$.

16
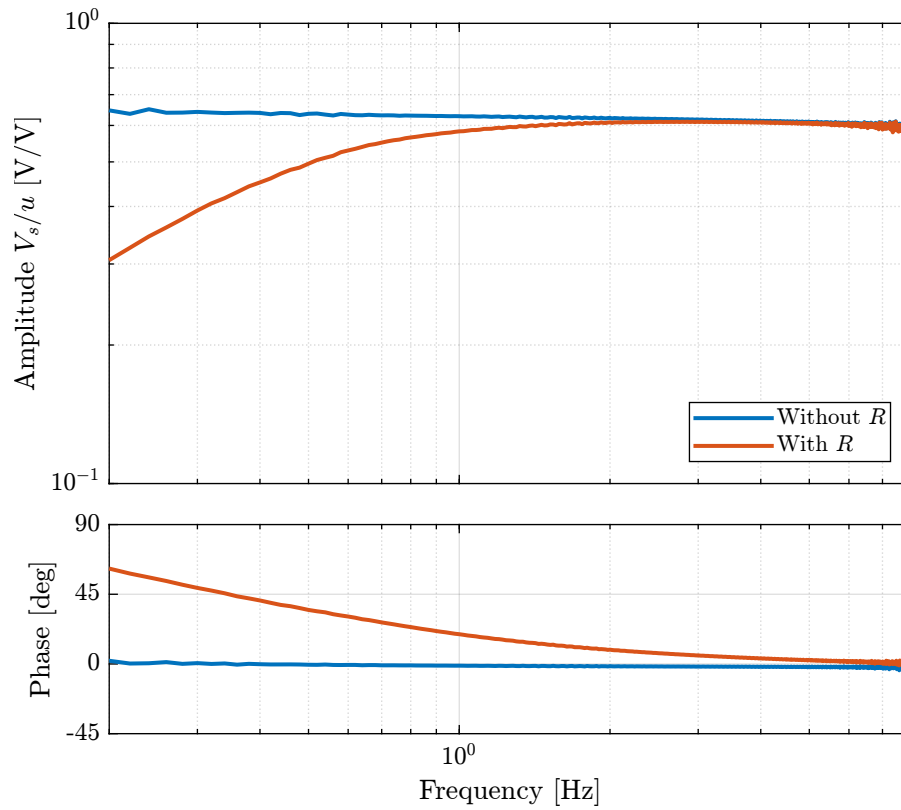
Figure 2.7: Transfer function from u to V_s with and without the resistor R in parallel with the piezo-electric stack used as the force sensor
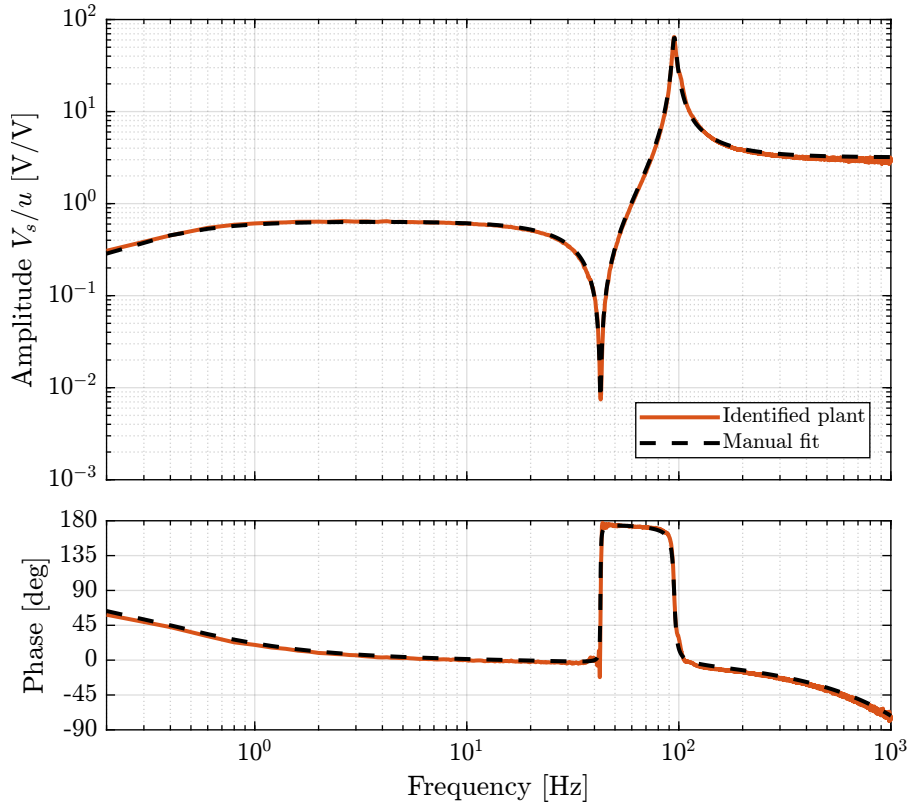
2.5 Integral Force Feedback

This test bench can also be used to estimate the damping added by the implementation of an Integral Force Feedback strategy.

First, the transfer function (2.3) is manually tuned to match the identified dynamics from generated voltage u to the measured sensor stack voltage V_s in Section 2.3.

The obtained parameter values are $\omega_{\text{HPF}} = 0.4\,\text{Hz}$, $\omega_z = 42.7\,\text{Hz}$, $\xi_z = 0.4\,\%$, $\omega_p = 95.2\,\text{Hz}$, $\xi_p = 2\,\%$ and $g_0 = 0.64$.

$$G_{\text{IFF},m}(s) = g_0 \cdot \frac{1 + 2\xi_z\frac{s}{\omega_z} + \frac{s^2}{\omega_z^2}}{1 + 2\xi_p\frac{s}{\omega_p} + \frac{s^2}{\omega_p^2}} \cdot \frac{s}{\omega_{\text{HPF}} + s} \tag{2.3}$$

The comparison between the identified plant and the manually tuned transfer function is done in Figure 2.8.

Figure 2.8: Identified IFF plant and manually tuned model of the plant (a time delay of $200\,\mu s$ is added to the model of the plant to better match the identified phase)

The implemented Integral Force Feedback Controller transfer function is shown in equation (2.4). It contains an high pass filter (cut-off frequency of $2\,\text{Hz}$) to limit the low frequency gain, a low pass filter to add integral action above $20\,\text{Hz}$, a second low pass filter to add robustness to high frequency resonances and a tunable gain g.

$$K_{\text{IFF}}(s) = -10 \cdot g \cdot \frac{s}{s + 2\pi \cdot 2} \cdot \frac{1}{1 + 2\pi \cdot 20} \cdot \frac{1}{s + 2\pi \cdot 2000} \tag{2.4}$$

To estimate how the dynamics of the APA changes when the Integral Force Feedback controller is implemented, the test bench shown in Figure 2.9 is used. The transfer function from the "damped" plant input $u\prime$ to the encoder displacement d_e is identified for several IFF controller gains g.
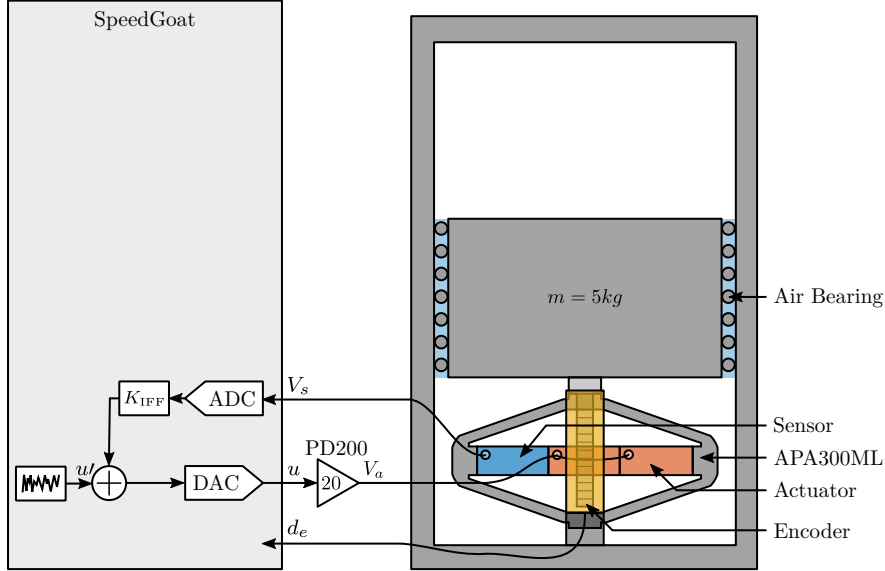

Figure 2.9: Figure caption

The identified dynamics are then fitted by second order transfer functions. The comparison between the identified damped dynamics and the fitted second order transfer functions is done in Figure 2.10 for different gains g. It is clear that large amount of damping is added when the gain is increased and that the frequency of the pole is shifted to lower frequencies.
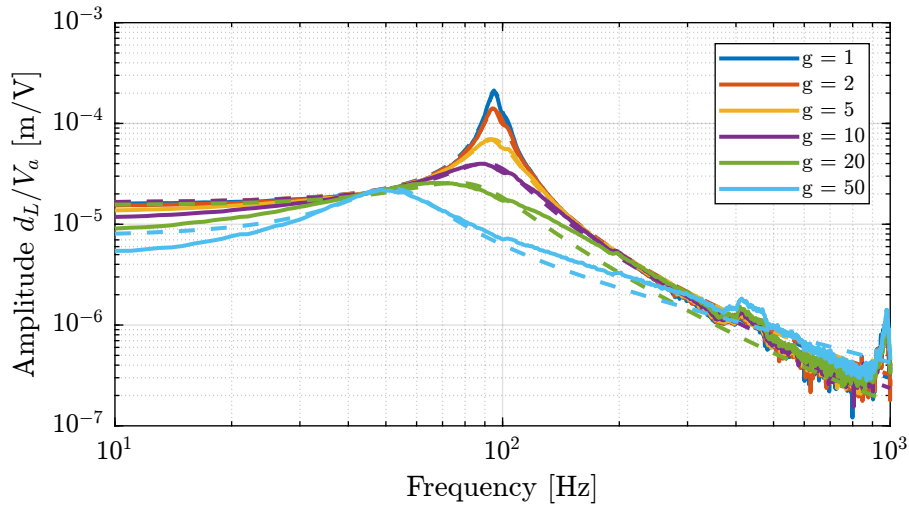

Figure 2.10: Identified dynamics (solid lines) and fitted transfer functions (dashed lines) from $u\prime$ to d_e for different IFF gains

The evolution of the pole in the complex plane as a function of the controller gain g (i.e. the "root locus") is computed:

- using the IFF plant model (2.3) and the implemented controller (2.4)

- from the fitted transfer functions of the damped plants experimentally identified for several controller gains

The two obtained root loci are compared in Figure 2.11 and are in good agreement considering that the damped plants were only fitted using a second order transfer function.
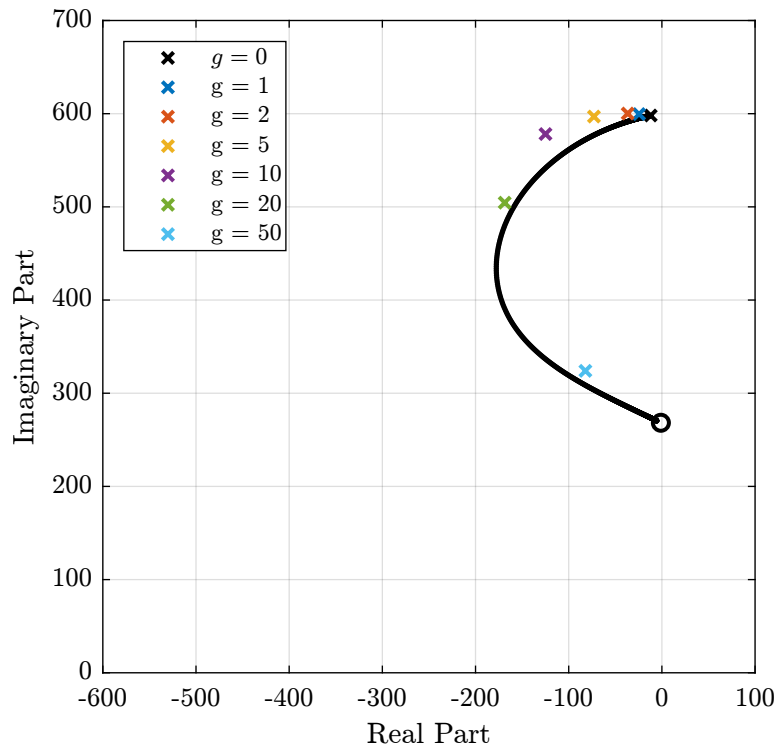
Figure 2.11: Root Locus of the APA300ML with Integral Force Feedback - Comparison between the computed root locus from the plant model (black line) and the root locus estimated from the damped plant pole identification (colorful crosses)

> **Important**
>
> So far, all the measured FRF are showing the dynamical behavior that was expected.

20

3 2 Degrees of Freedom Model

In this section, a simscape model (Figure 3.1) of the measurement bench is used to compare the model of the APA with the measured frequency response functions.

After the transfer functions are extracted from the model (Section **??**), the comparison of the obtained dynamics with the measured FRF will permit to:

1. Estimate the "actuator constant" and "sensor constant" (Section **??**)

2. "Actuator constant": Gain from the applied voltage V_a to the generated Force F_a

3. "Sensor constant": Gain from the sensor stack strain δL to the generated voltage V_s

4. Tune the model of the APA to match the measured dynamics (Section **??**)
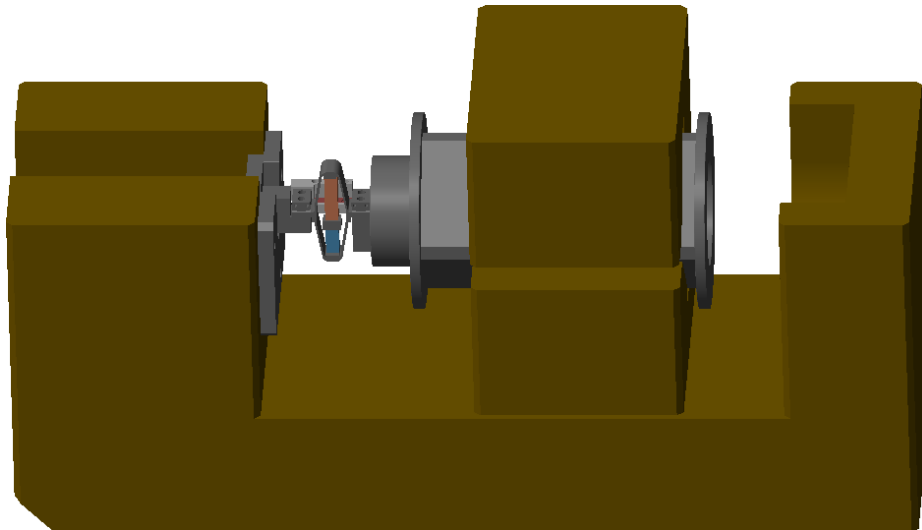

Figure 3.1: Screenshot of the Simscape model
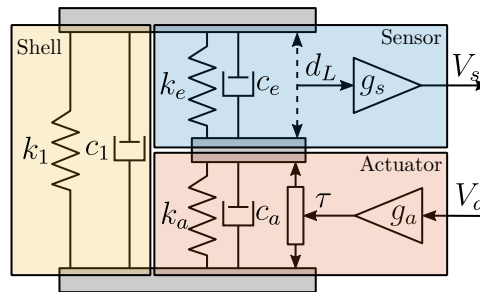
3.1 Two Degrees of Freedom APA Model

The APA model shown in Figure 3.2 is adapted from [2].

It can be decomposed into three components:

- the shell whose axial properties are represented by k_1 and c_1

- the actuator stacks whose contribution in the axial stiffness is represented by k_a and c_a. A force source τ represents the axial force induced by the force sensor stacks. The gain g_a (in N/m) is used to convert the applied voltage V_a to the axial force τ

- the actuator stacks whose contribution in the axial stiffness is represented by k_e and c_e. A "strain sensor" d_L, and a gain g_s (in V/m) that converts this strain into a generated voltage

Such simple model has some limitations:

- it only represents the axial characteristics of the APA (infinitely rigid in other directions)

- some physical insights are lost such as the amplification factor, the real stress and strain on the piezoelectric stacks

- it is fully linear and therefore the creep and hysteresis of the piezoelectric stacks are not modelled

Figure 3.2: Schematic of the two degrees of freedom model of the APA300ML

3.2 Tuning of the APA model

9 parameters (m, k_1, c_1, k_e, c_e, k_a, c_a, g_s and g_a) have to be tuned such that the dynamics of the model (Figure 3.3) well represents the identified dynamics in Section 2.
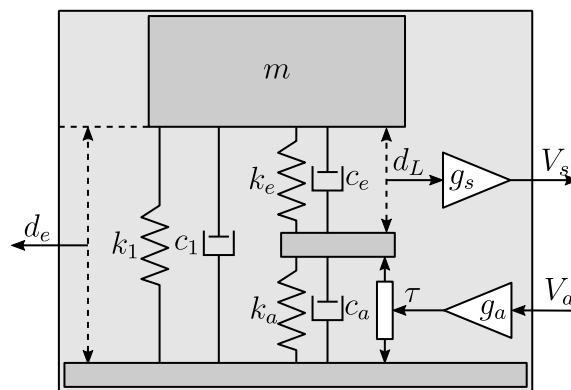
Figure 3.3: Schematic of the two degrees of freedom model of the APA300ML with input V_a and outputs d_e and V_s

First, the mass supported by the APA300ML can simply be estimated from the geometry and density of the different parts or by directly measuring it using a precise weighing scale. Both methods leads to an estimated mass of 5.7 kg.

Then, the axial stiffness of the shell was estimated at $k_1 = 0.38\,N/\mu m$ in Section 2.3 from the frequency of the anti-resonance seen on Figure 2.6. Similarly, c_1 can be estimated from the damping ratio of the same anti-resonance and is found to be close to $20\,Ns/m$.

Then, it is reasonable to make the assumption that the sensor stacks and the two actuator stacks have identical mechanical characteristics[1]. Therefore, we have $k_e = 2k_a$ and $c_e = 2c_a$ as the actuator stack is composed of two stacks in series. In that case, the total stiffness of the APA model is described by (3.1).

$$k_{\text{tot}} = k_1 + \frac{k_e k_a}{k_e + k_a} = k_1 + \frac{2}{3} k_a \tag{3.1}$$

Knowing from (3.2) that the total stiffness is $k_{\text{tot}} = 2\,N/\mu m$, we get from (3.1) that $k_a = 2.5\,N/\mu m$ and $k_e = 5\,N/\mu m$.

$$\omega_0 = \frac{k_{\text{tot}}}{m} \implies k_{\text{tot}} = m\omega_0^2 = 2\,N/\mu m \quad \text{with } m = 5.7\,\text{kg and } \omega_0 = 2\pi \cdot 95\,rad/s \tag{3.2}$$

Then, c_a (and therefore $c_e = 2c_a$) can be tuned to match the damping ratio of the identified resonance. $c_a = 100\,Ns/m$ and $c_e = 200\,Ns/m$ are obtained.

Finally, the two gains g_s and g_a can be used to match the gain of the identified transfer functions.

The obtained parameters of the model shown in Figure 3.3 are summarized in Table 3.1.

Table 3.1: Summary of the obtained parameters for the 2 DoF APA300ML model

Parameter	Value
m	$5.7\,\text{kg}$
k_1	$0.38\,N/\mu m$
k_e	$5.0\,N/\mu m$
k_a	$2.5\,N/\mu m$
c_1	$20\,Ns/m$
c_e	$200\,Ns/m$
c_a	$100\,Ns/m$
g_a	$-2.58\,N/V$
g_s	$4.6\,V/\mu m$

---

[1]Note that this is not fully correct as it was shown in Section 2.2 that the electrical boundaries of the piezoelectric stack impacts its stiffness and that the sensor stack is almost open-circuited while the actuator stacks are almost short-circuited.

3.3 Obtained Dynamics

The dynamics of the 2DoF APA300ML model is now extracted using optimized parameters (listed in Table 3.1) from the Simscape model. It is compared with the experimental data in Figure 3.4.

A good match can be observed between the model and the experimental data, both for the encoder and for the force sensor. This indicates that this model represents well the axial dynamics of the APA300ML.
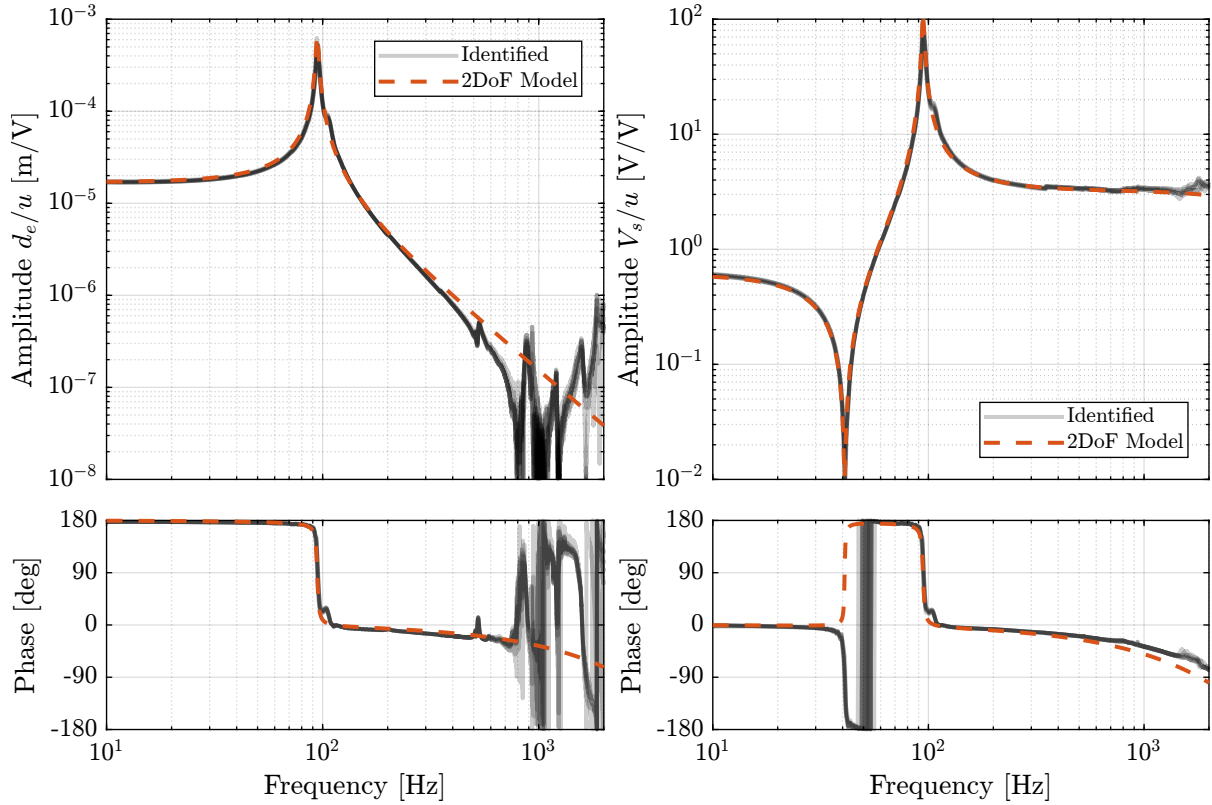

Figure 3.4: Comparison of the measured FRF and the optimized 2DoF model of the APA300ML

4 APA300ML – Super Element

In this section, a *super element* of the Amplified Piezoelectric Actuator "APA300ML" is extracted using a Finite Element Software. It is then imported in Simscape (using the stiffness and mass matrices) and it is included in the same model that was used in 3.

This procedure is illustrated in Figure 4.1.
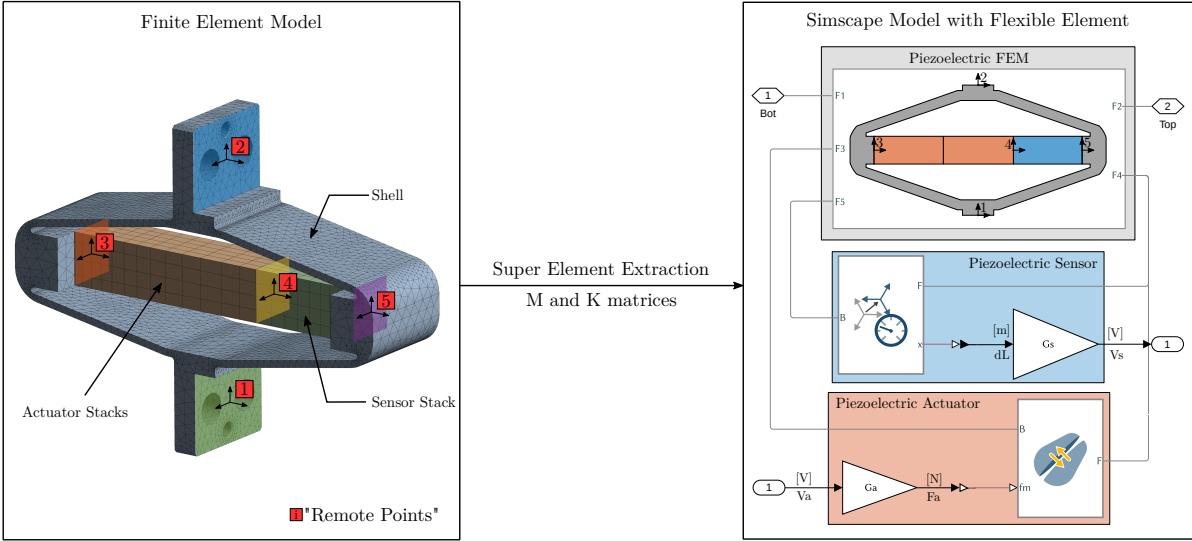
Figure 4.1: Finite Element Model of the APA300ML with "remotes points" on the left. Simscape model with included "Reduced Order Flexible Solid" on the right.

4.1 Extraction of the super-element

- Explain how the "remote points" are chosen

- Show some parts of the mass and stiffness matrices?

- Say which materials were used?

- Maybe this was already explain earlier in the manuscript

4.2 Identification of the Actuator and Sensor constants

Once the APA300ML *super element* is included in the Simscape model, the transfer function from F_a to d_L and d_e can be identified. The gains g_a and g_s can then be tuned such that the gain of the transfer functions are matching the identified ones.

By doing so, $g_s = 4.9\,V/\mu m$ and $g_a = 23.2\,N/V$ are obtained.

To make sure these "gains" are physically valid, it is possible to estimate them from physical properties of the piezoelectric stack material.

From [3, p. 123], the relation between relative displacement d_L of the sensor stack and generated voltage V_s is given by (4.1a) and from [4] the relation between the force F_a and the applied voltage V_a is given by (4.1b).

$$V_s = \underbrace{\frac{d_{33}}{\epsilon^T s^D n}}_{g_s} d_L \tag{4.1a}$$

$$F_a = \underbrace{d_{33} n k_a}_{g_a} \cdot V_a, \quad k_a = \frac{c^E A}{L} \tag{4.1b}$$

Parameters used in equations (4.1a) and (4.1b) are described in Table 4.1.

Unfortunately, the manufacturer of the stack was not willing to share the piezoelectric material properties of the stack used in the APA300ML. However, based on available properties of the APA300ML stacks in the data-sheet, the soft Lead Zirconate Titanate "THP5H" from Thorlabs seemed to match quite well the observed properties. The properties of this "THP5H" material used to compute g_a and g_s are listed in Table 4.1.

From these parameters, $g_s = 5.1\,V/\mu m$ and $g_a = 26\,N/V$ were obtained which are very close to the identified constants using the experimentally identified transfer functions.

Table 4.1: Piezoelectric properties used for the estimation of the sensor and actuators "gains"

Parameter	Value	Description
d_{33}	$680 \cdot 10^{-12}\,m/V$	Piezoelectric constant
ϵ^T	$4.0 \cdot 10^{-8}\,F/m$	Permittivity under constant stress
s^D	$21 \cdot 10^{-12}\,m^2/N$	Elastic compliance understand constant electric displacement
c^E	$48 \cdot 10^9\,N/m^2$	Young's modulus of elasticity
L	$20\,mm$ per stack	Length of the stack
A	$10^{-4}\,m^2$	Area of the piezoelectric stack
n	160 per stack	Number of layers in the piezoelectric stack

4.3 Comparison of the obtained dynamics

The obtained dynamics using the *super element* with the tuned "sensor gain" and "actuator gain" are compared with the experimentally identified frequency response functions in Figure 4.2.
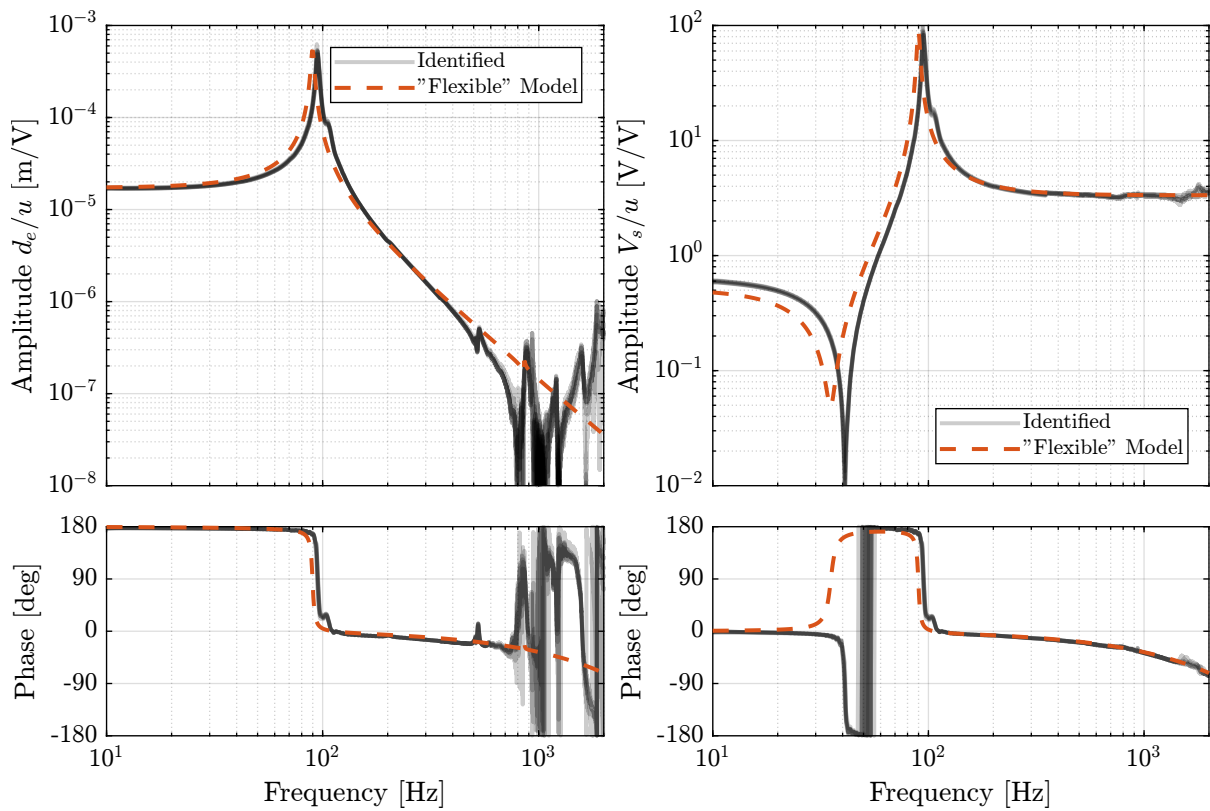
A good match between the model and the experimental results is observed.

- the *super element*

This model represents fairly

The flexible model is a bit "soft" as compared with the experimental results.

This method can be used to model piezoelectric stack actuators as well as amplified piezoelectric stack actuators.

Figure 4.2: Comparison of the measured FRF and the "Flexible" model of the APA300ML

5 Conclusion

- Compare 2DoF and FEM models (usefulness of the two)

- Good match between all the APA: will simplify the modeling and control of the nano-hexapod

- No advantage of the FEM model here (as only uniaxial behavior is checked), but may be useful later

Bibliography

[1]   M. Reza and F. Andrew, *Piezoelectric Transducers for Vibration Control and Damping.* London: Springer, 2006 (cit. on p. 14).

[2]   A. Souleille, T. Lampert, V. Lafarga, *et al.*, "A concept of active mount for space applications," *CEAS Space Journal*, vol. 10, no. 2, pp. 157–165, 2018 (cit. on p. 21).

[3]   A. J. Fleming and K. K. Leang, *Design, Modeling and Control of Nanopositioning Systems* (Advances in Industrial Control). Springer International Publishing, 2014 (cit. on p. 26).

[4]   A. J. Fleming and K. K. Leang, "Integrated strain and force feedback for high-performance control of piezoelectric actuators," *Sensors and Actuators A: Physical*, vol. 161, no. 1-2, pp. 256–265, 2010 (cit. on p. 26).